

Nonlinear response of cantilever beams to combination and subcombination resonances

Ali H. Nayfeh* and Haider N. Arafat

*Department of Engineering Science and Mechanics,
MC 0219, Virginia Polytechnic Institute and State
University, Blacksburg, VA 24061, USA*

Received 11 May 1998

Revised 18 September 1998

The nonlinear planar response of cantilever metallic beams to combination parametric and external subcombination resonances is investigated, taking into account the effects of cubic geometric and inertia nonlinearities. The beams considered here are assumed to have large length-to-width aspect ratios and thin rectangular cross sections. Hence, the effects of shear deformations and rotatory inertia are neglected. For the case of combination parametric resonance, a two-mode Galerkin discretization along with Hamilton's extended principle is used to obtain two second-order nonlinear ordinary-differential equations of motion and associated boundary conditions. Then, the method of multiple scales is applied to obtain a set of four first-order nonlinear ordinary-differential equations governing the modulation of the amplitudes and phases of the two excited modes. For the case of subcombination resonance, the method of multiple scales is applied directly to the Lagrangian and virtual-work term. Then using Hamilton's extended principle, we obtain a set of four first-order nonlinear ordinary-differential equations governing the amplitudes and phases of the two excited modes. In both cases, the modulation equations are used to generate frequency- and force-response curves. We found that the trivial solution exhibits a jump as it undergoes a subcritical pitchfork bifurcation. Similarly, the nontrivial solutions also exhibit jumps as they undergo saddle-node bifurcations.

Keywords: Beams, combination resonance, parametric resonance, subcombination resonance, bifurcations

1. Introduction

When a system is parametrically excited, combination parametric resonances may occur when the forc-

ing frequency $\Omega \approx \omega_i \pm \omega_j$, where ω_k is the natural frequency of the k th mode. When the excitation is direct, an external combination resonance can occur in systems with quadratic nonlinearities when $\Omega \approx \omega_i \pm \omega_j$ and in systems with cubic nonlinearities when $\Omega \approx |\omega_i \pm \omega_j \pm \omega_k|$ or $\Omega \approx |2\omega_i \pm \omega_j|$. An external subcombination resonance can occur when a forcing frequency is near one-half the sum or difference of two or more natural frequencies (Nayfeh and Mook [9]).

Dugundji and Mukhopadhyay [4] investigated the response of a thin cantilever metallic beam to combination parametric resonances involving the first bending and torsional modes (i.e., $\Omega \approx \omega_{B1} + \omega_{T1}$) in one case and the second bending and first torsional modes (i.e., $\Omega \approx \omega_{B2} + \omega_{T1}$) in another. Their experimental results show that the beam exhibits significant oscillations both in bending and in torsion. In addition, at large excitation amplitudes they observed the beam snapping-through and whipping around. Cartmell and Roberts [3] theoretically and experimentally investigated the stability of a cantilever beam-mass system possessing the two simultaneous combination parametric resonances $\Omega \approx \omega_{B1} + \omega_{T1} \approx \omega_{B2} - \omega_{T1}$. They analyzed their system using the method of multiple scales and found good agreement between theory and experiment within certain ranges of the excitation frequency. However, in other regions where periodic modulations can occur, the correlation was not satisfactory because the theoretical solution could not predict nonstationary responses.

Kar and Sujata [5] investigated the instability of an elastically restrained cantilever beam subjected to uniaxial and follower forces. They found that combination parametric resonances of the difference type do not occur when the force is uniaxial or supertangential, but that they are predominant when the force is tangential or subtangential. Kar and Sujata [6] also investigated the instability of a rotating, pretwisted, and preconed cantilever beam, taking into consideration the Coriolis effects. They found that the Coriolis force may increase the instability regions in the case of combination parametric resonances.

*Corresponding author. Tel.: +1 540 231 5453; Fax: +1 540 231 2290; E-mail: anayfeh@vt.edu.

Anderson et al. [1] experimentally investigated the response of a thin metallic cantilever beam with an initial curvature to a combination parametric excitation. The first four natural frequencies are 0.65 Hz, 5.65 Hz, 16.19 Hz, and 31.91 Hz. They found that, over a range of forcing frequency above 32 Hz, the first and fourth modes are activated by a combination parametric resonance with the first mode dominating the response.

Sridhar et al. [12] investigated the response of a hinged-clamped beam to the subcombination resonance $\Omega \approx \frac{1}{2}(\omega_a \pm \omega_b)$ and the combination resonance $\Omega \approx \omega_a \pm \omega_b \pm \omega_c$. Yamamoto et al. [16,17] theoretically and experimentally investigated the nonlinear response of simply-supported beams to combination and subcombination resonances, respectively. They [16] found that, in order to excite the external combination resonance, one needs a time-independent component in the excitation. However, they [17] found that the external subcombination resonance can be excited with only a harmonic excitation. In both cases, they found that only additive-type resonances can be activated. In these three studies, nonlinearities due to mid-plane stretching were included in the analysis.

The experimental results of Dugundji and Mukhopadhyay [4] and Anderson et al. [1] confirm the occurrence of such resonances in structures. More important, their results demonstrate that such resonances can be a mechanism where a high-frequency excitation can activate low-frequency large-amplitude modes. For example, the ratio of the excitation frequency to the natural frequency of lowest mode excited was approximately 18:1 in the experiments of Dugundji and Mukhopadhyay [4] and 49:1 in the experiments of Anderson et al. [1]. The analyses of Cartmell and Roberts [3] and Kar and Sujata [5,6] did not take into consideration the effect of nonlinearities inherent in the system.

In this paper, we investigate the response of a uniform thin metallic cantilever beam to either a combination parametric resonance or a subcombination resonance of two modes (see Fig. 1). Because such resonance phenomena cannot be adequately explained by using linear theories of vibrations, it is necessary to incorporate the effects of nonlinearities in the analysis. Furthermore, because the presence of a low-frequency component in the response may cause the beam to oscillate with large amplitudes, we account for both geometric and inertia nonlinearities. The method of multiple scales is used to determine two sets of four first-order nonlinear ordinary-differential equations governing the modulation of the amplitudes and phases of the

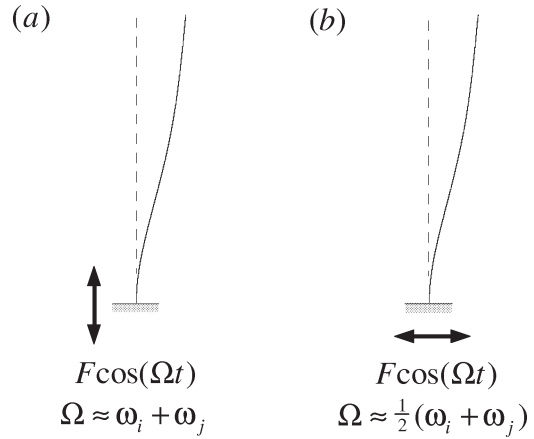


Fig. 1. A schematic of a cantilever beam under (a) combination parametric resonance and (b) external subcombination resonance.

two interacting modes. The modulation equations are then used to generate frequency- and force-response curves.

2. Combination parametric resonance

The nondimensional equation of motion for inextensional cantilever beams where the effects of shear deformation and rotatory inertia are neglected is given by

$$\begin{aligned} \ddot{v} + c\dot{v} + v^{iv} = & -(v'^2 v'''' + v'v''^2)' \\ & - \frac{1}{2} \left(v' \frac{\partial^2}{\partial t^2} \int_1^s \int_0^s v'^2 ds ds \right)' \\ & + F(s, v) \cos(\Omega t), \end{aligned} \quad (1)$$

where the dimensional time $t^* = t\sqrt{mL^4/EI}$ and the dimensional deflection and arc-length are $v^* = Lv$ and $s^* = Ls$. The boundary conditions are

$$v = 0 \quad \text{and} \quad v' = 0 \quad \text{at} \quad s = 0, \quad (2)$$

$$v'' = 0 \quad \text{and} \quad v''' = 0 \quad \text{at} \quad s = 1. \quad (3)$$

The corresponding nondimensional Lagrangian and virtual work are given by

$$\begin{aligned} \mathcal{L} = \int_0^1 \left\{ \frac{1}{2} \dot{v}^2 + \frac{1}{2} \left(\frac{1}{2} \frac{\partial}{\partial t} \int_0^s v'^2 ds \right)^2 \right. \\ \left. - \frac{1}{2} (v''^2 + v'^2 v''^2) \right\} ds, \end{aligned} \quad (4)$$

$$\delta W = \int_0^1 Q_v \delta v ds$$

$$= \int_0^1 \{F(s, v) \cos(\Omega t) - c\dot{v}\} \delta v \, ds, \quad (5)$$

where the prime denotes differentiation with respect to the arclength s and the dot denotes differentiation with respect to time t . Eqs (1)–(5) are valid for beams that are uniform, homogeneous, long, and thin. For stubby or thick beams, shear deformation and rotatory inertia effects may not be negligible (Timoshenko [14]).

In the presence of damping, all of the modes that are not directly excited or indirectly excited by an internal resonance will decay with time. Hence, for the case of combination parametric resonance or external subcombination resonance of the m th and n th modes, where the ϕ_i are the orthonormal mode shapes, the long-time response of the beam will consist only of these two modes if neither of them is involved in an internal resonance with any other mode. Therefore, we assume a solution for v in the form

$$v(s, t) = \phi_m(s)\eta_m(t) + \phi_n(s)\eta_n(t). \quad (6)$$

For cantilever beams,

$$\phi_i(s) = c_i \left\{ \cosh(z_i s) - \cos(z_i s) + \frac{\cos(z_i) + \cosh(z_i)}{\sin(z_i) + \sinh(z_i)} [\sin(z_i s) - \sinh(z_i s)] \right\}, \quad (7)$$

where z_i is the i th root of $1 + \cos(z) \cosh(z) = 0$ and c_i is chosen so that $\int_0^1 \phi_i^2 \, ds = 1$. The nondimensional natural frequencies are given by

$$\omega_i = z_i^2. \quad (8)$$

The first four nondimensional frequencies are $\omega_1 = 3.5160$, $\omega_2 = 22.0345$, $\omega_3 = 61.6972$, and $\omega_4 = 120.9019$.

For the case of combination parametric resonance, we let

$$F(s, v) = -[v''(s-1) + v']f. \quad (9)$$

Substituting Eqs (6)–(9) into Eqs (4) and (5) and integrating the result over space, we obtain the discretized Lagrangian and virtual work as

$$\mathcal{L} = \frac{1}{2} (1 + \delta_1 \eta_m^2 + 2\delta_2 \eta_m \eta_n + \delta_3 \eta_n^2) \dot{\eta}_m^2$$

$$+ \frac{1}{2} (1 + \delta_4 \eta_m^2 + 2\delta_5 \eta_m \eta_n + \delta_6 \eta_n^2) \dot{\eta}_n^2 + (\delta_7 \eta_m^2 + \delta_8 \eta_m \eta_n + \delta_9 \eta_n^2) \dot{\eta}_m \dot{\eta}_n - \frac{1}{2} (\omega_m^2 \eta_m^2 + \omega_n^2 \eta_n^2) - \alpha_1 \eta_m^4 - \alpha_2 \eta_m^3 \eta_n - \alpha_3 \eta_m^2 \eta_n^2 - \alpha_4 \eta_m \eta_n^3 - \alpha_5 \eta_n^4, \quad (10)$$

$$\delta W = -[2\mu_m \dot{\eta}_m + (f_{mm} \eta_m + f_{mn} \eta_n) \cos(\Omega t)] \delta \eta_m - [2\mu_n \dot{\eta}_n + (f_{nm} \eta_m + f_{nn} \eta_n) \cos(\Omega t)] \delta \eta_n = Q_m \delta \eta_m + Q_n \delta \eta_n, \quad (11)$$

where the δ_i , α_i , μ_i , and f_{ij} are defined in Appendix A.

By applying Hamilton's extended principle,

$$\frac{d}{dt} \left(\frac{\partial \mathcal{L}}{\partial \dot{\eta}_m} \right) - \frac{\partial \mathcal{L}}{\partial \eta_m} = Q_m, \quad (12)$$

$$\frac{d}{dt} \left(\frac{\partial \mathcal{L}}{\partial \dot{\eta}_n} \right) - \frac{\partial \mathcal{L}}{\partial \eta_n} = Q_n, \quad (13)$$

we obtain

$$\begin{aligned} & \ddot{\eta}_m + 2\mu_m \dot{\eta}_m + \omega_m^2 \eta_m \\ &= -(4\alpha_1 \eta_m^3 + 3\alpha_2 \eta_m^2 \eta_n + 2\alpha_3 \eta_m \eta_n^2 + \alpha_4 \eta_n^3) \\ & \quad - (\delta_1 \eta_m^2 + 2\delta_2 \eta_m \eta_n + \delta_3 \eta_n^2) \ddot{\eta}_m \\ & \quad - (\delta_7 \eta_m^2 + \delta_8 \eta_m \eta_n + \delta_9 \eta_n^2) \ddot{\eta}_n \\ & \quad - (\delta_1 \eta_m + \delta_2 \eta_n) \dot{\eta}_m^2 - 2(\delta_2 \eta_m + \delta_3 \eta_n) \dot{\eta}_m \dot{\eta}_n \\ & \quad - [(\delta_8 - \delta_4) \eta_m + (2\delta_9 - \delta_5) \eta_n] \dot{\eta}_n^2 \\ & \quad - (f_{mm} \eta_m + f_{mn} \eta_n) \cos(\Omega t), \end{aligned} \quad (14)$$

$$\begin{aligned} & \ddot{\eta}_n + 2\mu_n \dot{\eta}_n + \omega_n^2 \eta_n \\ &= -(\alpha_2 \eta_m^3 + 2\alpha_3 \eta_m^2 \eta_n + 3\alpha_4 \eta_m \eta_n^2 + 4\alpha_5 \eta_n^3) \\ & \quad - (\delta_7 \eta_m^2 + \delta_8 \eta_m \eta_n + \delta_9 \eta_n^2) \ddot{\eta}_m \\ & \quad - (\delta_4 \eta_m^2 + 2\delta_5 \eta_m \eta_n + \delta_6 \eta_n^2) \ddot{\eta}_n \\ & \quad - [(2\delta_7 - \delta_2) \eta_m + (\delta_8 - \delta_3) \eta_n] \dot{\eta}_m^2 \\ & \quad - 2(\delta_4 \eta_m + \delta_5 \eta_n) \dot{\eta}_m \dot{\eta}_n \\ & \quad - (\delta_5 \eta_m + \delta_6 \eta_n) \dot{\eta}_n^2 \\ & \quad - (f_{nm} \eta_m + f_{nn} \eta_n) \cos(\Omega t). \end{aligned} \quad (15)$$

To determine a second-order uniform expansion for the solutions of Eqs (14) and (15) for the case of com-

combination parametric resonance of the additive type, we scale μ_i and f_{ij} as $\varepsilon^2\mu_i$ and ε^2f_{ij} and introduce the detuning parameter σ so that

$$\Omega = \omega_m + \omega_n + \varepsilon^2\sigma, \quad (16)$$

where ε is a small nondimensional bookkeeping parameter. Next, using the method of multiple scales (Nayfeh [7]), we obtain

$$\eta_m = \varepsilon [A_m(T_2)e^{i\omega_m T_0} + \bar{A}_m(T_2)e^{-i\omega_m T_0}] + \dots, \quad (17)$$

$$\eta_n = \varepsilon [A_n(T_2)e^{i\omega_n T_0} + \bar{A}_n(T_2)e^{-i\omega_n T_0}] + \dots, \quad (18)$$

where $T_0 = t$, $T_2 = \varepsilon^2 t$, and A_m and A_n are governed by

$$\begin{aligned} -2i\omega_m(A'_m + \mu_m A_m) &= S_{mm}A_m^2\bar{A}_m \\ &+ S_{mn}A_m A_n \bar{A}_n + \frac{1}{2}f_{mn}\bar{A}_n e^{i\sigma T_2}, \end{aligned} \quad (19)$$

$$\begin{aligned} -2i\omega_n(A'_n + \mu_n A_n) &= S_{nn}A_n^2\bar{A}_n \\ &+ S_{nm}A_n A_m \bar{A}_m + \frac{1}{2}f_{nm}\bar{A}_m e^{i\sigma T_2}, \end{aligned} \quad (20)$$

the prime indicates the derivative with respect to T_2 , and

$$\begin{aligned} S_{mm} &= 12\alpha_1 - 2\omega_m^2\delta_1, \\ S_{nn} &= 12\alpha_5 - 2\omega_n^2\delta_6, \\ S_{mn} &= S_{nm} = 4\alpha_3 - 2\omega_m^2\delta_3 - 2\omega_n^2\delta_4. \end{aligned} \quad (21)$$

The S_{ij} and f_{ij} were calculated for combination parametric resonances of the additive type for different pairs of the first four modes. The results are shown in Table 1. It follows from Table 1 that $S_{11} > 0$ and S_{22} , S_{33} , and $S_{44} < 0$. Hence, the nonlinearity is of the hardening type for the first mode and of the softening type for the higher modes.

The complex-valued modulation equations (19) and (20) can be transformed into a real-valued form by introducing the transformation

$$A_m = \frac{1}{2}a_m e^{i\beta_m} \quad \text{and} \quad A_n = \frac{1}{2}a_n e^{i\beta_n}. \quad (22)$$

Substituting Eqs (22) into Eqs (19) and (20) and separating real and imaginary parts, we obtain

$$a'_m = -\mu_m a_m - \frac{f_{mn}}{4\omega_m} a_n \sin \gamma, \quad (23)$$

$$\begin{aligned} a_m \beta'_m &= \frac{S_{mm}}{8\omega_m} a_m^3 + \frac{S_{mn}}{8\omega_m} a_m a_n^2 \\ &+ \frac{f_{mn}}{4\omega_m} a_n \cos \gamma, \end{aligned} \quad (24)$$

$$a'_n = -\mu_n a_n - \frac{f_{nm}}{4\omega_n} a_m \sin \gamma, \quad (25)$$

$$a_n \beta'_n = \frac{S_{nm}}{8\omega_n} a_m^2 a_n + \frac{S_{nn}}{8\omega_n} a_n^3 + \frac{f_{nm}}{4\omega_n} a_m \cos \gamma, \quad (26)$$

where

$$\gamma \equiv \sigma T_2 - \beta_m - \beta_n. \quad (27)$$

Substituting Eqs (22) into Eqs (17) and (18) and then substituting the result into Eq. (6), we find that the beam response is given by

$$\begin{aligned} v(s, t) &\approx \varepsilon [a_m \phi_m(s) \cos(\omega_m t + \beta_m) \\ &+ a_n \phi_n(s) \cos(\omega_n t + \beta_n)], \end{aligned} \quad (28)$$

where the a_i and β_i are given by Eqs (23)–(27). Using Eqs (16) and (27) to eliminate ω_n and β_n from Eq. (28), we have

$$\begin{aligned} v(s, t) &\approx \varepsilon \{ a_m \phi_m(s) \cos(\omega_m t + \beta_m) \\ &+ a_n \phi_n(s) \cos[(\Omega - \omega_m)t - \beta_m - \gamma] \}. \end{aligned} \quad (29)$$

The equilibrium solutions or fixed points of Eqs (23)–(27) correspond to $a'_m = 0$, $a'_n = 0$, and $\gamma' = 0$, which in turn correspond to two-period quasiperiodic responses of the beam according to Eq. (29). There are two possible equilibrium solutions: (a) $a_m = 0$ and $a_n = 0$ and the beam is not excited and (b) $a_m \neq 0$ and $a_n \neq 0$ and the beam response is quasiperiodic. In the latter case, Eqs (24), (26), and (27) can be used to eliminate β_m and β_n to obtain the following equation for γ :

$$\begin{aligned} \gamma' &= \sigma - \left(\frac{S_{mm}}{8\omega_m} + \frac{S_{nm}}{8\omega_n} \right) a_m^2 - \left(\frac{S_{mn}}{8\omega_m} + \frac{S_{nn}}{8\omega_n} \right) a_n^2 \\ &- \left(\frac{a_n f_{mn}}{4a_m \omega_m} + \frac{a_m f_{nm}}{4a_n \omega_n} \right) \cos \gamma. \end{aligned} \quad (30)$$

Thus, for nontrivial solutions, the modulation equations are reduced from four to three first-order differential equations. For equilibrium solutions, we set the

Table 1

Values of the coefficients α_i , δ_i , S_{ij} , and f_{ij} for different combinations of the first four modes

Modes m & n	S_{mm}	$S_{mn} = S_{nm}$	S_{nn}
1 & 2	7.6680	-1122.2408	-100279.6731
1 & 3	7.6680	-15928.9047	-6818871.8310
2 & 3	-100279.6731	-75835.2975	-6818871.8310
1 & 4	7.6680	-34594.5220	-1.1042 $\times 10^8$
2 & 4	-100279.6731	-927411.9209	-1.1042 $\times 10^8$
3 & 4	-6818871.8310	-4017517.1670	-1.1042 $\times 10^8$
Modes m & n	f_{mm}	$f_{mn} = f_{nm}$	f_{nn}
1 & 2	1.5709 <i>f</i>	-0.4223 <i>f</i>	8.6471 <i>f</i>
1 & 3	1.5709 <i>f</i>	-1.0721 <i>f</i>	24.9521 <i>f</i>
2 & 3	8.6471 <i>f</i>	1.8901 <i>f</i>	24.9521 <i>f</i>
1 & 4	1.5709 <i>f</i>	-0.8731 <i>f</i>	51.4591 <i>f</i>
2 & 4	8.6471 <i>f</i>	-3.6434 <i>f</i>	51.4591 <i>f</i>
3 & 4	24.9521 <i>f</i>	8.3383 <i>f</i>	51.4591 <i>f</i>

time derivatives in Eqs (23), (25), and (30) equal to zero and solve for a_m , a_n , and γ , yielding the following closed-form solution:

$$\alpha_e a_m^2 = \sigma \pm \frac{\mu_m + \mu_n}{\sqrt{\mu_m \mu_n}} \sqrt{\frac{f_{mn} f_{nm}}{16 \omega_m \omega_n} - \mu_m \mu_n}, \quad (31)$$

$$a_n^2 = \frac{\mu_m \omega_m f_{nm}}{\mu_n \omega_n f_{mn}} a_m^2, \quad (32)$$

$$\begin{aligned} \sin \gamma &= -\frac{4 \mu_m \omega_m a_m}{f_{mn} a_n} = -\frac{4 \mu_n \omega_n a_n}{f_{nm} a_m} \\ &= \pm 4 \sqrt{\frac{\mu_m \mu_n \omega_m \omega_n}{f_{mn} f_{nm}}}, \end{aligned} \quad (33)$$

where

$$\begin{aligned} \alpha_e &= \frac{1}{8} \left[\frac{S_{mm}}{\omega_m} + \frac{S_{nm}}{\omega_n} \right. \\ &\quad \left. + \left(\frac{S_{mn}}{\omega_m} + \frac{S_{nn}}{\omega_n} \right) \frac{\mu_m \omega_m f_{nm}}{\mu_n \omega_n f_{mn}} \right]. \end{aligned} \quad (34)$$

The stability of a nontrivial equilibrium solution can then be studied by calculating the eigenvalues of the Jacobian matrix of Eqs (23), (25), and (30) evaluated at this equilibrium solution.

To determine the stability of the trivial equilibrium solutions, we study the stability of the linearized complex-valued modulation equations (19) and (20). To this end, we let

$$A_m = c_m e^{\lambda T_2 + i \sigma T_2} \quad \text{and} \quad A_n = c_n e^{\bar{\lambda} T_2} \quad (35)$$

in the linearized equations (19) and (20) and obtain

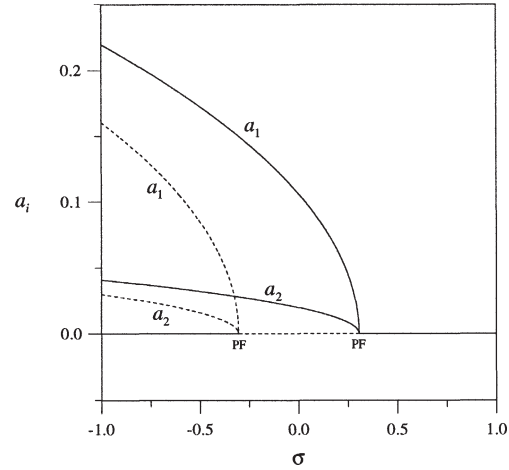


Fig. 2. Frequency-response curves for a combination parametric resonance of the additive type involving modes 1 and 2 for $f = 10$, $\mu_1 = 0.0137$, $\mu_2 = 0.0635$. Solid lines (—) denote stable fixed points and dashed lines (---) denote unstable fixed points.

$$2i \omega_m (\lambda + i \sigma + \mu_m) c_m + \frac{1}{2} f_{mn} \bar{c}_n = 0, \quad (36)$$

$$2i \omega_n (\bar{\lambda} + \mu_n) c_n + \frac{1}{2} f_{nm} \bar{c}_m = 0. \quad (37)$$

Hence,

$$\begin{aligned} \lambda &= -\frac{1}{2} (\mu_m + \mu_n + i \sigma) \pm \left(\frac{1}{4} (\mu_m + \mu_n + i \sigma)^2 \right. \\ &\quad \left. - \mu_n (\mu_m + i \sigma) + \frac{f_{mn} f_{nm}}{16 \omega_m \omega_n} \right)^{1/2}. \end{aligned} \quad (38)$$

It follows from Eqs (35) that the trivial solution is sta-

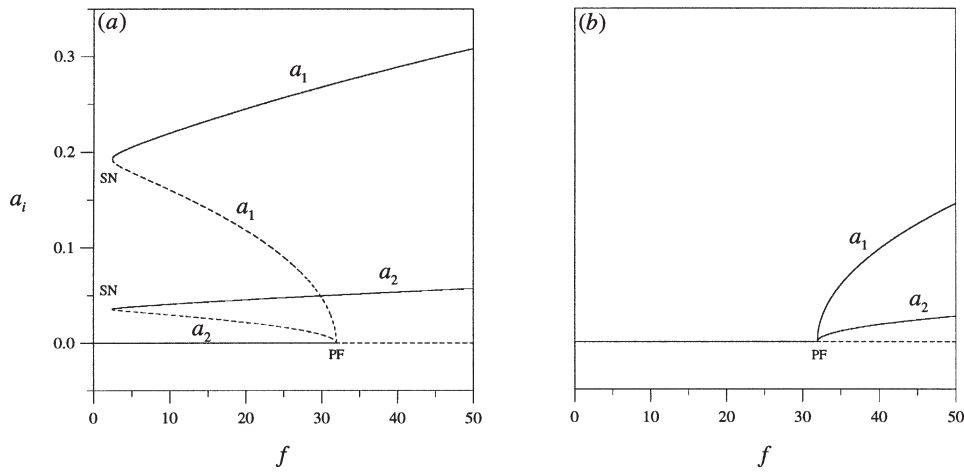


Fig. 3. Amplitude-response curves for a combination parametric resonance of the additive type involving modes 1 and 2 when $\mu_1 = 0.0137$ and $\mu_2 = 0.0635$. In part (a), $\sigma = -1$ and in part (b), $\sigma = 1$. Solid lines (—) denote stable fixed points and dashed lines (---) denote unstable fixed points.

ble if the real parts of both λ 's are negative.

In Fig. 2, we show typical frequency-response curves for a combination parametric resonance of the additive type of the first two modes when the excitation amplitude is $f = 10$. Clearly, the first mode dominates the response. Although the nonlinearity is hardening for the first mode and softening for the second mode, the frequency-response curves are bent to the left, indicating a softening behavior for both modes. This is so because

$$\beta'_1 = \frac{S_{11}}{8\omega_1} a_1^2 + \frac{S_{12}}{8\omega_1} a_2^2 + \frac{f_{12}a_2}{4\omega_1 a_1} \cos \gamma \quad (39)$$

according to Eq. (24). Although S_{11} is positive, S_{12} is negative and its magnitude is much larger than S_{11} . Hence, the nonlinearity decreases the frequency of the first mode, and hence bends the frequency-response curves to the left. It follows from Fig. 2 that, depending on how σ is varied, the trivial solution loses stability via either a subcritical or a supercritical pitchfork bifurcation.

In Fig. 3, we show amplitude-response curves for a combination parametric resonance of the additive type of the first two modes. In part (a), the frequency detuning parameter $\sigma = -1$, and in part (b) $\sigma = 1$. When $\sigma = -1$, there are two branches of nontrivial fixed-point solutions, one stable and the other unstable. As f is increased away from zero, the trivial solution loses stability via a subcritical pitchfork bifurcation, causing the response to jump up to the stable branch of nontrivial solutions. Similarly, a fixed-point on the stable nontrivial branch loses stability via a saddle-node bifurca-

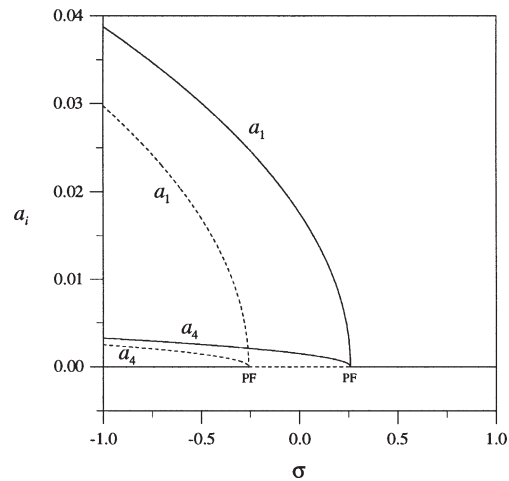


Fig. 4. Frequency-response curves for a combination parametric resonance of the additive type involving modes 1 and 4 for $f = 10$, $\mu_1 = 0.0137$, $\mu_4 = 0.0573$. Solid lines (—) denote stable fixed points and dashed lines (---) denote unstable fixed points.

tion as f is decreased, resulting in a jump down to the trivial branch. When $\sigma \geq 0$, there are only branches of stable nontrivial fixed points, as shown in Fig. 3(b). The nontrivial solution is activated gradually as the trivial solution undergoes a supercritical pitchfork bifurcation.

In Figs 4 and 5, the frequency- and amplitude-response curves are presented when the first and fourth modes are activated by the combination parametric resonance. The forcing amplitude in Fig. 4 is $f = 10$ and the detuning parameter is $\sigma = -1$ in Fig. 5(a) and $\sigma = 1$ in Fig. 5(b). We note that the behaviors in Figs 4 and 5 are similar to those in Figs 2 and 3. However, the

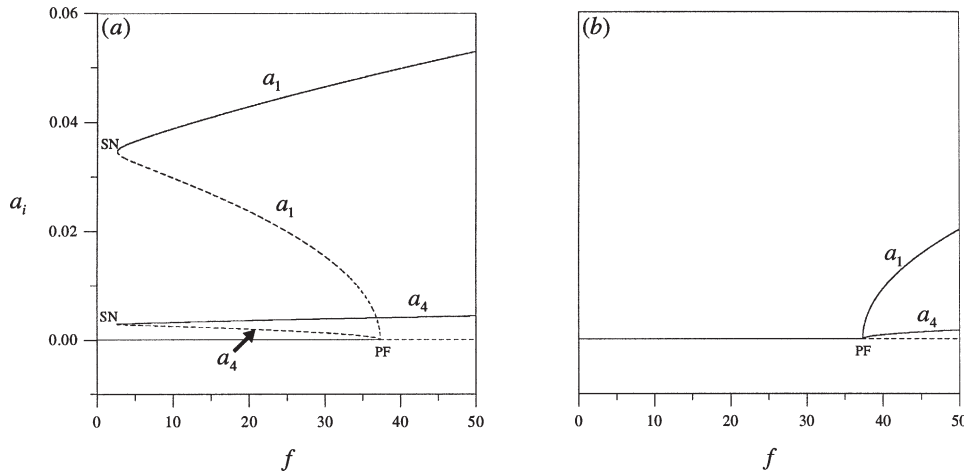


Fig. 5. Amplitude-response curves for a combination parametric resonance of the additive type involving modes 1 and 4 when $\mu_1 = 0.0137$ and $\mu_4 = 0.0573$. In part (a), $\sigma = -1$ and in part (b), $\sigma = 1$. Solid lines (—) denote stable fixed points and dashed lines (---) denote unstable fixed points.

amplitudes when modes 1 and 4 are excited are about an order of magnitude smaller than those when modes 1 and 2 are excited.

Anderson et al. [1] experimentally investigated the response of a cantilever beam where $\Omega \approx 2\omega_3 \approx \omega_1 + \omega_4$. They found that over a small region of frequency detuning, only the first and fourth modes were excited by a combination parametric resonance. The results shown in Fig. 4 agree qualitatively with their frequency-response curves.

Results for the case of a combination parametric resonance of the difference type can be obtained by replacing ω_m by $-\omega_m$ and β_m by $-\beta_m$ in Eqs (23)–(32). However, it can be seen from Eq. (32) that this resonance cannot be activated in this system.

3. External subcombination resonance

In this section, we consider the response of the beam to the subcombination resonance $\Omega \approx \frac{1}{2}(\omega_n \pm \omega_m)$. In this case, the excitation, which is transverse, is assumed to be hard. Therefore, we let $F(s, v) = \varepsilon f(s)$ in Eqs (1) and (5). Furthermore, in order that the cubic nonlinearities and damping balance the resonance, we scale c as $\varepsilon^2 c$. We use the method of time-averaged Lagrangian and virtual work to determine a uniform first-order expansion. To this end, we let

$$v(s, T_0, T_2) \approx \varepsilon [A_m(T_2)\phi_m(s)e^{i\omega_m T_0} + A_n(T_2)\phi_n(s)e^{i\omega_n T_0} + \Phi(s)e^{i\Omega T_0} + cc], \quad (40)$$

where $\phi_m(s)$ and $\phi_n(s)$ are the mode shapes corresponding to the natural frequencies ω_m and ω_n and $\Phi(s)$ is governed by the boundary-value problem

$$\Phi^{iv} - \Omega^2 \Phi = \frac{1}{2} f(s), \quad (41)$$

$$\begin{aligned} \Phi(0) = 0, \quad \Phi'(0) = 0, \\ \Phi''(1) = 0, \quad \text{and} \quad \Phi'''(1) = 0. \end{aligned} \quad (42)$$

We note that $2\varepsilon\Phi(s) \cos(\Omega t)$ is the particular solution of the linear undamped beam equation and associated boundary conditions. When $f(s)$ is constant, the solution of Eqs (41) and (42) can be expressed as

$$\begin{aligned} \Phi(s) = c_1 \sin(\sqrt{\Omega} s) + c_2 \cos(\sqrt{\Omega} s) \\ + c_3 \sinh(\sqrt{\Omega} s) \\ + c_4 \cosh(\sqrt{\Omega} s) - \frac{f}{2\Omega^2}, \end{aligned} \quad (43)$$

where

$$c_1 = -c_3 = \frac{f}{4\Omega^2} \frac{\sin \sqrt{\Omega} \cosh \sqrt{\Omega} + \cos \sqrt{\Omega} \sinh \sqrt{\Omega}}{1 + \cos \sqrt{\Omega} \cosh \sqrt{\Omega}}, \quad (44)$$

$$c_2 = \frac{f}{4\Omega^2} \frac{1 + \cos \sqrt{\Omega} \cosh \sqrt{\Omega} - \sin \sqrt{\Omega} \sinh \sqrt{\Omega}}{1 + \cos \sqrt{\Omega} \cosh \sqrt{\Omega}}, \quad (45)$$

$$c_4 = \frac{f}{4\Omega^2} \frac{1 + \cos \sqrt{\Omega} \cosh \sqrt{\Omega} + \sin \sqrt{\Omega} \sinh \sqrt{\Omega}}{1 + \cos \sqrt{\Omega} \cosh \sqrt{\Omega}}. \quad (46)$$

Clearly, Eqs (44)–(46) break down when Ω is near any of the natural frequencies of the beam. In the present case, $\Omega \approx \frac{1}{2}(\omega_m \pm \omega_n)$, which is away from any of the natural frequencies.

Next, we introduce the detuning parameter σ such that

$$\Omega = \frac{1}{2}(\omega_m + \omega_n) + \varepsilon^2 \sigma. \quad (47)$$

Substituting Eq. (40) into Eqs (4) and (5), using Eq. (47), and retaining only slowly varying terms, we obtain the following time-averaged Lagrangian and virtual work:

$$\begin{aligned} \frac{\langle \mathcal{L} \rangle}{\varepsilon^4} &= i\omega_m (A_m \bar{A}'_m - \bar{A}_m A'_m) \\ &+ i\omega_n (A_n \bar{A}'_n - \bar{A}_n A'_n) - \Gamma_m A_m \bar{A}_m \\ &- \Gamma_n A_n \bar{A}_n - \frac{1}{2} S_{mm} A_m^2 \bar{A}_m^2 \\ &- \frac{1}{2} S_{nn} A_n^2 \bar{A}_n^2 - S_{mn} A_m \bar{A}_m A_n \bar{A}_n \\ &- \Lambda (\bar{A}_m \bar{A}_n e^{2i\sigma T_2} + A_m A_n e^{-2i\sigma T_2}) \\ &+ \text{constant} + \dots, \end{aligned} \quad (48)$$

$$\begin{aligned} \frac{\langle \delta W \rangle}{\varepsilon^4} &= -2i\omega_m \mu_m (A_m \delta \bar{A}_m - \bar{A}_m \delta A_m) \\ &- 2i\omega_n \mu_n (A_n \delta \bar{A}_n - \bar{A}_n \delta A_n) + \dots, \end{aligned} \quad (49)$$

where the S_{ij} are defined in Eqs (21), the μ_i are defined in Appendix A, and Γ_m, Γ_n , and Λ are defined in Appendix B. In Table 2, we present the numerical values for the coefficients Γ_m, Γ_n , and Λ for external subcombination resonances of the additive type for different pairs of the first four modes. Applying Hamilton's principle to Eqs (48) and (49), we obtain the modulation equations

$$\begin{aligned} -2i\omega_m (A'_m + \mu_m A_m) &= \Gamma_m A_m + S_{mm} A_m^2 \bar{A}_m \\ &+ S_{mn} A_m A_n \bar{A}_n + \Lambda \bar{A}_n e^{2i\sigma T_2}, \end{aligned} \quad (50)$$

$$\begin{aligned} -2i\omega_n (A'_n + \mu_n A_n) &= \Gamma_n A_n + S_{nm} A_m \bar{A}_m A_n \\ &+ S_{nn} A_n^2 \bar{A}_n + \Lambda \bar{A}_m e^{2i\sigma T_2}. \end{aligned} \quad (51)$$

Substituting the polar transformation, Eqs (22), into Eqs (50) and (51) and separating real and imaginary

Table 2

Values of the coefficients Γ_m, Γ_n , and Λ for different combinations of the first four modes

Modes m & n	Γ_m	Γ_n	Λ
1 & 2	$-0.0107f^2$	$-0.1268f^2$	$0.0130f^2$
1 & 3	$-0.0005f^2$	$-0.0420f^2$	$0.0051f^2$
2 & 3	$-0.0111f^2$	$-0.0531f^2$	$0.0006f^2$
1 & 4	$-0.0588f^2$	$-15.3290f^2$	$0.9893f^2$
2 & 4	$-0.0045f^2$	$-0.0298f^2$	$0.0161f^2$
3 & 4	$-0.0135f^2$	$-0.0420f^2$	$-0.0041f^2$

parts, we obtain the real-valued modulation equations

$$a'_m = -\mu_m a_m - \frac{\Lambda}{2\omega_m} a_n \sin \gamma, \quad (52)$$

$$\begin{aligned} a_m \beta'_m &= \frac{\Gamma_m}{2\omega_m} a_m + \frac{S_{mm}}{8\omega_m} a_m^3 \\ &+ \frac{S_{mn}}{8\omega_m} a_m a_n^2 + \frac{\Lambda}{2\omega_m} a_n \cos \gamma, \end{aligned} \quad (53)$$

$$a'_n = -\mu_n a_n - \frac{\Lambda}{2\omega_n} a_m \sin \gamma, \quad (54)$$

$$\begin{aligned} a_n \beta'_n &= \frac{\Gamma_n}{2\omega_n} a_n + \frac{S_{nm}}{8\omega_n} a_m^2 a_n \\ &+ \frac{S_{nn}}{8\omega_n} a_n^3 + \frac{\Lambda}{2\omega_n} a_m \cos \gamma, \end{aligned} \quad (55)$$

where

$$\gamma \equiv 2\sigma T_2 - \beta_m - \beta_n. \quad (56)$$

We note that, except for the linear shifts $\Gamma_i/2\omega_i$ in the natural frequencies, Eqs (52)–(56) have the same form as Eqs (23)–(27) obtained for the case of combination parametric resonance if we put $f_{mn} = 2\Lambda$ and replace σ with 2σ .

There are two possible solutions for Eqs (52)–(56): (a) $a_m = a_n = 0$ and (b) $a_m \neq 0$ and $a_n \neq 0$. In the first case, it follows from Eq. (40) that the beam's response is given by

$$v(s, t) = 2\varepsilon \Phi(s) \cos(\Omega t) + \dots, \quad (57)$$

which is periodic having the same period as that of the excitation. In this case, the external subcombination resonance is not activated. The stability of this trivial solution can be analyzed by investigating solutions of the linearized complex-valued modulation equations (50) and (51). To this end, we let

$$A_m = c_m e^{\lambda T_2 + 2i\sigma T_2} \quad \text{and} \quad A_n = c_n e^{\bar{\lambda} T_2} \quad (58)$$

in the linearized equations (50) and (51) and obtain

$$\left[2i\omega_m(\mu_m + \lambda + 2i\sigma) + \Gamma_m\right]c_m + \Lambda\bar{c}_n = 0, \quad (59)$$

$$\Lambda\bar{c}_m + \left[2i\omega_n(\mu_n + \bar{\lambda}) + \Gamma_n\right]c_n = 0. \quad (60)$$

For nontrivial solutions,

$$\begin{aligned} \lambda^2 + \left[(\mu_m + \mu_n) + i\left(2\sigma - \frac{\Gamma_m}{2\omega_m} + \frac{\Gamma_n}{2\omega_n}\right)\right]\lambda \\ + \left[\left(\mu_m\mu_n - \frac{\sigma\Gamma_n}{\omega_n} + \frac{\Gamma_m\Gamma_n - \Lambda^2}{4\omega_m\omega_n}\right) \right. \\ \left. + i\left(2\sigma\mu_n - \frac{\Gamma_m\mu_n}{2\omega_m} + \frac{\Gamma_n\mu_m}{2\omega_n}\right)\right] = 0. \end{aligned} \quad (61)$$

It follows from Eqs (58) that the trivial solution loses stability as one of the λ 's crosses the imaginary axis along the real axis from the left-half to the right-half of the complex plane.

For nontrivial solutions, we use Eqs (53), (55), and (56) to eliminate β_m and β_n and obtain

$$\begin{aligned} \gamma' = 2\sigma - \frac{1}{2}\left(\frac{\Gamma_m}{\omega_m} + \frac{\Gamma_n}{\omega_n}\right) \\ - \frac{1}{8}\left(\frac{S_{mm}}{\omega_m} + \frac{S_{nm}}{\omega_n}\right)a_m^2 \\ - \frac{1}{8}\left(\frac{S_{mn}}{\omega_m} + \frac{S_{nn}}{\omega_n}\right)a_n^2 \\ - \frac{\Lambda}{2}\left(\frac{a_n}{\omega_m a_m} + \frac{a_m}{\omega_n a_n}\right)\cos\gamma. \end{aligned} \quad (62)$$

The fixed points of Eqs (52), (54), and (62) correspond to $a'_m = 0$, $a'_n = 0$, and $\gamma' = 0$. They are given by

$$\begin{aligned} \alpha_e a_m^2 = 2\sigma - \frac{1}{2}\left(\frac{\Gamma_m}{\omega_m} + \frac{\Gamma_n}{\omega_n}\right) \\ \pm \frac{\mu_m + \mu_n}{\sqrt{\mu_m\mu_n}} \sqrt{\frac{\Lambda^2}{4\omega_m\omega_n} - \mu_m\mu_n}, \end{aligned} \quad (63)$$

$$a_n^2 = \frac{\mu_m\omega_m}{\mu_n\omega_n} a_m^2, \quad (64)$$

$$\sin\gamma = -\frac{2\mu_m\omega_m}{\Lambda} \frac{a_m}{a_n} = -\frac{2\mu_n\omega_n}{\Lambda} \frac{a_n}{a_m}, \quad (65)$$

$$\begin{aligned} \cos\gamma = \left[2\sigma - \frac{1}{2}\left(\frac{\Gamma_m}{\omega_m} + \frac{\Gamma_n}{\omega_n}\right) \right. \\ \left. - \frac{1}{8}\left(\frac{S_{mm}}{\omega_m} + \frac{S_{nm}}{\omega_n}\right)a_m^2 \right. \end{aligned}$$

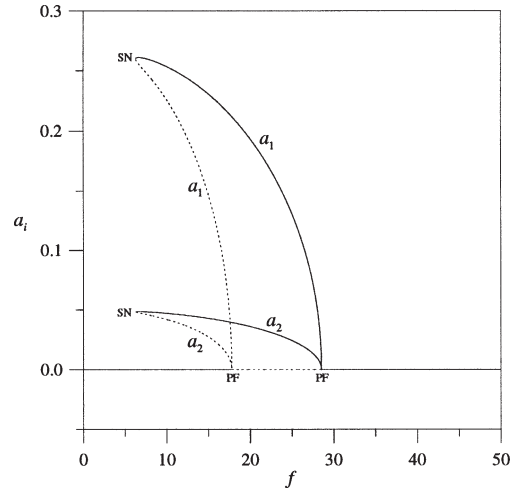


Fig. 6. Amplitude-response curves for an additive-type external subcombination resonance involving modes 1 and 2 for $\sigma = -1$, $\mu_1 = 0.0137$ and $\mu_2 = 0.0635$. Solid lines (—) denote stable fixed points and dashed lines (---) denote unstable fixed points.

$$\begin{aligned} - \frac{1}{8}\left(\frac{S_{mn}}{\omega_m} + \frac{S_{nn}}{\omega_n}\right)a_n^2 \\ \times \left[\frac{\Lambda}{2}\left(\frac{a_n}{\omega_m a_m} + \frac{a_m}{\omega_n a_n}\right)\right]^{-1}, \end{aligned} \quad (66)$$

where

$$\alpha_e = \frac{1}{8}\left[\frac{S_{mm}}{\omega_m} + \frac{S_{nm}}{\omega_n} + \left(\frac{S_{mn}}{\omega_m} + \frac{S_{nn}}{\omega_n}\right)\frac{\mu_m\omega_m}{\mu_n\omega_n}\right]. \quad (67)$$

In Fig. 6, we show typical amplitude-response curves for the subcombination external resonance of the first two modes for $\sigma = -1$. The trivial solution loses stability via a subcritical pitchfork bifurcation as the forcing amplitude is increased, resulting in a jump in the response amplitudes. On the other hand, as the forcing amplitude is decreased from a large value, the trivial solution loses stability through a supercritical pitchfork bifurcation, resulting in a gradual increase in the response amplitudes. In either case, the nontrivial solution loses stability as f is decreased via a saddle-node bifurcation. Comparing Figs 3 and 6, we conclude that the linear shift in the natural frequencies $\Gamma_i/2\omega_i$ and the nonlinear dependence of the effective forcing Λ ($\Lambda \propto f^2$) on the excitation amplitude have dramatic qualitative and quantitative effects on the force-response curves.

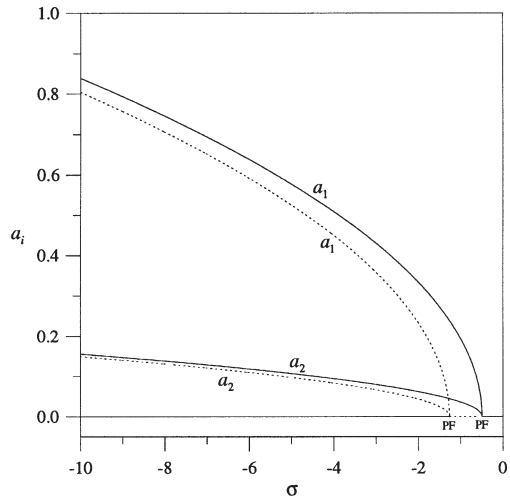


Fig. 7. Frequency-response curves for an additive-type external subcombination resonance involving modes 1 and 2 for $f = 20$, $\mu_1 = 0.0137$ and $\mu_2 = 0.0635$. Solid lines (—) denote stable fixed points and dashed lines (---) denote unstable fixed points.

In Fig. 7, we show typical frequency-response curves for the same resonance when $f = 20$. As in the case of combination parametric resonance, the curves are bent to the left, indicating a softening-type nonlinearity. Because Γ_1 and Γ_2 are negative and proportional to f^2 , there is a strong decrease in the linear natural frequencies with an increase in f . Consequently, for $f = 20$, unlike the combination parametric resonance, the external subcombination resonance is activated only for negative values of σ . We also note that increasing the forcing amplitude causes both the stable and unstable branches to shift to the left, with the latter being shifted more than the former.

In Fig. 8, we show typical amplitude-response curves for a subcombination external resonance of the first and third modes for $\sigma = -1$. Comparing Figs 6 and 8, we note that the amplitude-response curves for the external subcombination resonance of modes 1 and 3 are qualitatively different from the amplitude-response curves for the external subcombination resonance of modes 1 and 2. As in Fig. 6, the trivial solution in Fig. 8 loses stability via a subcritical pitchfork bifurcation as f is increased, resulting in a jump in the response amplitudes. However, the amplitudes of the nontrivial solutions in Fig. 8 increase as f is increased, in contrast to the results in Fig. 6, where the amplitudes of the nontrivial solutions decrease as f is increased.

Comparing Figs 3(a) and 5(a) with Fig. 8, we note that the amplitude-response curves for the external subcombination resonance of modes 1 and 3 are similar to those obtained for the combination parametric

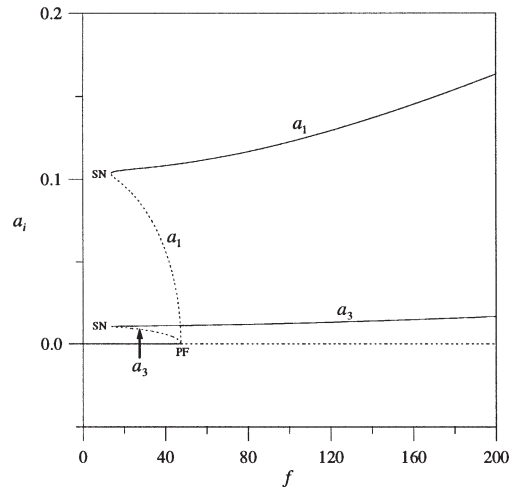


Fig. 8. Amplitude-response curves for an additive-type external subcombination resonance involving modes 1 and 3 for $\sigma = -1$, $\mu_1 = 0.0137$ and $\mu_3 = 0.076$. Solid lines (—) denote stable fixed points and dashed lines (---) denote unstable fixed points.

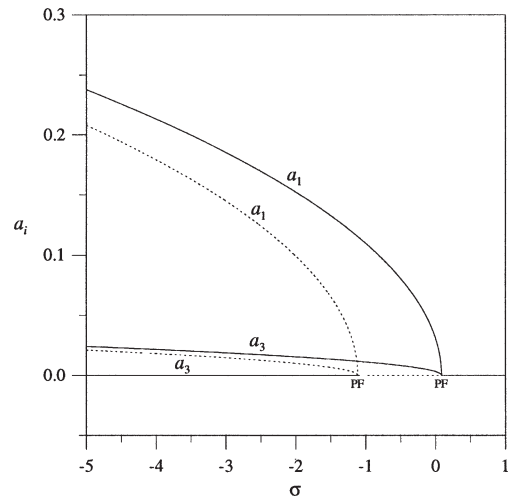


Fig. 9. Frequency-response curves for an additive-type external subcombination resonance involving modes 1 and 3 for $f = 50$, $\mu_1 = 0.0137$ and $\mu_3 = 0.076$. Solid lines (—) denote stable fixed points and dashed lines (---) denote unstable fixed points.

resonance. Therefore, the effects of the linear shifts in the natural frequencies and the nonlinear dependence of the effective forcing Λ on the excitation amplitude f do not change qualitatively the amplitude-response curves.

In Fig. 9, we show typical frequency-response curves for the external subcombination resonance of modes 1 and 3 when $f = 50$. Again the curves are bent to the left, indicating that the nonlinearity and the linear shift $\Gamma_1/2\omega_1$ decrease the frequency of the dominant first

mode. Furthermore, similar to the combination parametric resonance, this case of external subcombination resonance may be activated for positive as well as negative values of σ .

Of the cases mentioned in Table 2, we found that the responses obtained for the external subcombination resonance of modes 2 and 4 are qualitatively similar to those obtained for the external subcombination resonance of modes 1 and 3, whereas the behaviors of the remaining cases are qualitatively similar to the external subcombination resonance of modes 1 and 2.

Finally, we note again that the case of external subcombination resonance of the difference type can be studied by replacing ω_m by $-\omega_m$ and β_m by $-\beta_m$ in Eqs (52)–(56). However, it can be seen from Eq. (64) that this resonance cannot be activated.

4. Conclusion

The nonlinear flexural responses of cantilever beams to combination parametric and subcombination resonances have been investigated. For the case of combination parametric resonance, the beam is excited longitudinally, whereas for the case of external subcombination resonance, the beam is excited transversely. In the parametric case, the Lagrangian and virtual-work term are discretized using a two-mode Galerkin technique and Hamilton's extended principle is used to obtain two second-order nonlinear ordinary-differential equations of motion. Then, the method of multiple scales is used to obtain a set of four first-order nonlinear ordinary-differential equations governing the modulation of the amplitudes and phases of the two excited modes. In the subcombination case, the method of time-averaged Lagrangian and virtual work along with Hamilton's extended principle are used to obtain the modulation equations.

We found that the excitation amplitude must exceed a certain threshold for either resonance to be activated. For the external subcombination resonance, two qualitatively different amplitude-response behaviors were found. In the first, the external subcombination resonance will not be activated if the excitation amplitude is chosen beyond a certain limit. In the second, similar to the case of combination parametric resonance, no upper limit on the excitation amplitude exists for the resonance to be activated.

In both parametric combination and external subcombination resonances, the trivial solution loses stability via pitchfork bifurcations, both supercritical and

subcritical, thereby producing nontrivial responses. When the pitchfork bifurcation is supercritical, the change in amplitudes is gradual and therefore the transition is smooth. When the pitchfork bifurcation is subcritical, the change in amplitudes is abrupt and is associated with a jump. In addition, the nontrivial solutions lose stability via saddle-node bifurcations as the excitation amplitude is decreased below a critical value, resulting in a jump down to the trivial solution.

For cantilever beams, we found that combination parametric and external subcombination resonances of the difference type cannot be activated. Rather, only additive-type resonances can be excited.

Acknowledgment

This work was supported by the National Science Foundation under Grant No. CMS-9423774.

Appendix A

$$\delta_1 = \int_0^1 \left(\int_0^s \phi_m'^2 ds \right)^2 ds,$$

$$\delta_2 = \delta_7 = \int_0^1 \left(\int_0^s \phi_m'^2 ds \right) \left(\int_0^s \phi_m' \phi_n' ds \right) ds,$$

$$\delta_3 = \delta_4 = \int_0^1 \left(\int_0^s \phi_m' \phi_n' ds \right)^2 ds,$$

$$\delta_5 = \delta_9 = \int_0^1 \left(\int_0^s \phi_m' \phi_n' ds \right) \left(\int_0^s \phi_n'^2 ds \right) ds,$$

$$\delta_6 = \int_0^1 \left(\int_0^s \phi_n'^2 ds \right)^2 ds,$$

$$\delta_8 = \delta_3 + \int_0^1 \left(\int_0^s \phi_m'^2 ds \right) \left(\int_0^s \phi_n'^2 ds \right) ds,$$

$$\alpha_1 = \frac{1}{2} \int_0^1 \phi_m'^2 \phi_m''^2 ds,$$

$$\alpha_2 = \int_0^1 (\phi_m'^2 \phi_m'' \phi_n'' + \phi_m' \phi_m''^2 \phi_n') ds,$$

$$\alpha_3 = \frac{1}{2} \int_0^1 (\phi_m''^2 \phi_n'^2 + 4\phi_m' \phi_m'' \phi_n' \phi_n'' + \phi_m'^2 \phi_n''^2) ds,$$

$$\alpha_4 = \int_0^1 (\phi'_m \phi'_n \phi''_n + \phi''_m \phi''_n \phi'_n) \, ds,$$

$$\alpha_5 = \frac{1}{2} \int_0^1 \phi''_n \phi''_n \, ds,$$

$$\mu_i = \frac{1}{2} \int_0^1 c \phi_i^2 \, ds,$$

$$f_{ij} = \int_0^1 [\phi''_i (s-1) + \phi'_i] \phi_j f \, ds, \quad i, j = m, n.$$

Appendix B

$$\Gamma_i = \int_0^1 \left[2\phi_i'' \Phi'^2 + 8\phi_i' \phi_i'' \Phi' \Phi'' + 2\phi_i^2 \Phi''^2 - 2(\omega_i^2 + \Omega^2) \left(\int_0^s \phi_i' \Phi' \, ds \right)^2 \right] ds,$$

$$\Lambda = \int_0^1 \left[2\phi'_m \phi''_n \Phi' \Phi'' + 2\phi''_m \phi'_n \Phi' \Phi'' + \phi'_m \phi'_n \Phi''^2 + \phi''_m \phi''_n \Phi'^2 + (\Omega^2 + \omega_m \omega_n - \omega_m \Omega - \omega_n \Omega) \times \left(\int_0^s \phi'_m \Phi' \, ds \right) \left(\int_0^s \phi'_n \Phi' \, ds \right) - \Omega(\omega_m + \omega_n) \times \left(\int_0^s \phi'_m \phi'_n \, ds \right) \left(\int_0^s \Phi'^2 \, ds \right) \right] ds.$$

References

- [1] T.J. Anderson, B. Balachandran and A.H. Nayfeh, Nonlinear resonances in a flexible cantilever beam, *J. Vibration and Acoustics, Trans. ASME* **116** (1994), 480–484.
- [2] K.G. Asmis and W.K. Tso, Combination and internal resonance in a nonlinear two-degrees-of-freedom system, *J. Applied Mechanics, Trans. ASME* **39** (1972), 832–834.
- [3] M.P. Cartmell and J.W. Roberts, Simultaneous combination resonances in a parametrically excited cantilever beam, *Strain* **23** (1987), 117–126.
- [4] J. Dugundji and V. Mukhopadhyay, Lateral bending–torsion vibrations of a thin beam under parametric excitation, *J. Applied Mechanics, Trans. ASME* **40** (1973), 693–698.
- [5] R.C. Kar and T. Sujata, Parametric instability of an elastically restrained cantilever beam, *Computers and Structures* **34** (1990), 469–475.
- [6] R.C. Kar and T. Sujata, Dynamic stability of a rotating, pretwisted and preconed cantilever beam including coriolis effects, *Computers & Structures* **42** (1992), 741–750.
- [7] A.H. Nayfeh, *Introduction to Perturbation Techniques*, Wiley-Interscience, New York, 1981.
- [8] A.H. Nayfeh, Combination resonances in the non-linear response of bowed structures to a harmonic excitation, *J. Sound and Vibration* **90** (1983), 457–470.
- [9] A.H. Nayfeh and D.T. Mook, *Nonlinear Oscillations*, Wiley-Interscience, New York, 1979.
- [10] A.H. Nayfeh and L.D. Zavodney, The response of two-degree-of-freedom systems with quadratic non-linearities to a combination parametric resonance, *J. Sound and Vibration* **107** (1986), 329–350.
- [11] J. Shaw, S.W. Shaw and A.G. Haddow, On the response of the non-linear vibration absorber, *Int. J. Non-Linear Mechanics* **24** (1989), 281–293.
- [12] S. Sridhar, A.H. Nayfeh and D.T. Mook, Nonlinear resonances in a class of multi-degree-of-freedom systems, *J. Acoustical Society of America* **58** (1975), 113–123.
- [13] D.A. Streit, A.K. Bajaj and C.M. Krousgrill, Combination parametric resonance leading to periodic and chaotic response in two-degree-of-freedom systems with quadratic non-linearities, *J. Sound and Vibration* **124** (1988), 297–314.
- [14] S. Timoshenko, *Vibration Problems in Engineering*, Van Nostrand, New York, 1928.
- [15] W.K. Tso and K.G. Asmis, Multiple parametric resonance in a non-linear two degree of freedom system, *Int. J. Non-Linear Mechanics* **9** (1974), 269–277.
- [16] T. Yamamoto, K. Yasuda and N. Tei, Summed and differential harmonic oscillations in a slender beam, *Bulletin JSME* **24** (1981), 1214–1222.
- [17] T. Yamamoto, K. Yasuda and N. Tei, Super summed and differential harmonic oscillations in a slender beam, *Bulletin JSME* **25** (1982), 959–968.